will cause an increase in reactance, however. For $2\ a/\lambda = 1.8$, for example, the reactance first decreases slightly and then increases as the dielectric thickness is increased from $D/a = 0$ to $D/a = 0.1$.

V. Conclusions

The application of the spectral domain method to the analysis of a fin-line resonator has been described. It has been shown the equivalent reactance of a bifurcating septum may be found by this method. Numerical and experimental data for septum reactance have been presented and have been shown to be in quite good agreement. Since the fin-line wavelength, λ', is used in the calculation of the septum reactance, the results presented here also provide an indirect verification of the accuracy of the wavelength calculations described in [3]. Selected design curves have been presented which should cover many cases encountered in practice.

The successful use of the spectral-domain approach in solving the septum discontinuity problem treated here suggests that the method should prove useful in solving a variety of planar line discontinuity problems.

Acknowledgment

The author wishes to acknowlege the contribution of LT. Guy Miller, U.S. Navy who supervised the design of the experimental apparatus and provided some of the experimental data reported here.

References

[1] J. B. Knorr and K-D. Kuchler, "Analysis of coupled slots and coplanar strips on dielectric substrate," *IEEE Trans. Microwave Theory Tech.*, vol. MTT-23, pp. 541–548, July 1975.

[2] J. B. Knorr and A. Tufekcioglu, "Spectral-domain calculation of microstrip characteristics impedance," *IEEE Trans. Microwave Theory Tech.*, vol. MTT-23, pp. 725–728, Sept. 1975.

[3] J. B. Knorr and P. M. Shayda, "Millimeter-wave fin-line characteristics," *IEEE Trans. Microwave Theory Tech.*, vol. MTT-28, pp. 737–743, July 1980.

[4] T. Itoh, "Analysis of microstrip resonators," *IEEE Trans. Microwave Theory Tech.*, vol. MTT-22, pp. 946–962, Nov. 1974.

[5] R. Harrington, *Time Harmonic Electromagnetic Fields*. New York: McGraw-Hill, 1961.

[6] N. Marcuvitz, *Waveguide Handbook*. New York: McGraw-Hill, 1951.

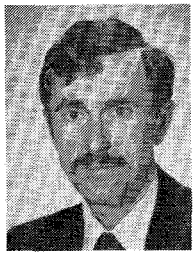

Jeffrey B. Knorr (S'68–M'71) was born in Lincoln Park, NJ, on May 8, 1940. He received the B.S. and M.S. degrees in electrical engineering from Pennsylvania State University, University Park, in 1963 and 1964, respectively, and the Ph.D. degree in electrical engineering from Cornell University, Ithaca, NY, in 1970.

From 1964 to 1967 he served with the U.S. Navy. In September 1970, he joined the faculty of the Naval Postgraduate School, Monterey, CA, where he currently holds the rank of Associate Professor in the Department of Electrical Engineering. He is also a member of the interdisciplinary Electronic Warfare Academic Group which is responsible for the administration of the Electronic Warfare Curriculum at the Naval Postgraduate School.

Dr. Knorr is a member of Sigma Xi.

Energy Absorption from Small Radiating Coaxial Probes in Lossy Media

MAYS L. SWICORD SENIOR MEMBER, IEEE, AND CHRISTOPHER C. DAVIS

***Abstract*—This paper describes the calculation of energy deposition around small open-ended coaxial antenna probes in lossy media. Two theoretical methods, a small monopole approximation (I) and an equivalent magnetic current source (II), are evaluated and compared. Method I is shown to be inappropriate for determining near field energy deposition. Power contour plots determined by method II in the vicinity of the open-ended coaxial antenna are presented as well as calculations of total power absorbed as a function of distance from the antenna center for various antenna dimensions and media dielectric properties. Our calculations of absorbed power distributions near the antenna are consistent with the limited experimental data which is available for comparison. A frequency of 2.45 GHz was selected for these calculations so that the results will be of value to workers interested in the application of open-ended coaxial antennas for invasive treatment of cancer by microwave hyperthermia.**

Manuscript received March 6, 1981; revised June 29, 1981.

M. L. Swicord is with the Bureau of Radiological Health, Rockville, MD 20857.

C. C. Davis is with the Electrical Engineering Department, University of Maryland, College Park, MD 20742.

I. Introduction

CALCULATIONS of field distributions and energy deposition around small open-ended coaxial probes in lossy media have been made and are reported here. Such small probes have been used or proposed for use in dielectrometry, hyperthermic treatment of small tumors and microwave spectroscopic investigations of liquids. The results of this investigation are instructive in all of the above cases, but will, it is hoped, be particularly helpful to those

0018-9480/81/1100-1202$00.75 ©1981 IEEE

interested in invasive antenna probes for cancer therapy by microwave hyperthermia. Although the design of probes for this application has varied depending upon the desired use, such probes are frequently open-ended coaxial transmission lines with a flush end or with the center conductor extending beyond the outer conductor by an amount which is always a small fraction of a wavelength in the medium. The authors' interest stems from the use of the former type of probe for coupling microwave energy into dielectric media and the subsequent observation of absorption as a function of frequency with an optical heterodyne technique [1]. It had been hoped that calculations of the near fields of such probes would yield fields which decayed with distance from the antenna in a way which could be approximated by some relatively simple analytic function. The results of these calculations did not support this hope but did lead to the adoption of a new irradiation scheme [2] which was amenable to analytic description.

Although several investigations [3]–[6] have reported temperature profiles produced in lossy media in which open-ended coaxial probes are immersed, these data do not reflect near-field distributions well because of the effects of thermal conduction. No measurements of the near fields of such small probes have been reported—even the best miniature E-field probes [7] are insufficiently small to allow near-field mapping of a miniature implantable probe. Consequently we felt that a realistic theoretical analysis of the near fields of such a probe would be of value. To the best of our knowledge such an analysis has not been given previously. Burdette *et al.* [8] discussed a model which is appropriate for such an analysis, namely the open-ended coaxial line opening into a ground plane where the region between the inner conductor and ground plane is replaced by an equivalent magnetic current sheet. However, these authors only restated the far field of such an antenna in a lossless medium [9], [10], viz.,

$$H_\phi = -\frac{\omega\epsilon\pi V \sin\theta (b^2-a^2) e^{-j\beta r}}{2\lambda r \ln(b/a)} \tag{1}$$

where the geometry of the open-ended coaxial line is given in Fig. 1. ω is the angular frequency, $\beta = 2\pi/\lambda$ is the wavenumber, λ is the wavelength, and $E_\theta = ZH_\phi$.

Apart from a constant of proportionality, the fields given by (1) are identical to those for the far field of an infinitesimal monopole

$$H_\phi = \frac{j\beta I\, dl \sin\theta e^{-j\beta r}}{2\pi r} \tag{2}$$

where I is the current amplitude in the monopole and dl is its length. The fields predicted by (1) and (2), which we will call the "infinitesimal monopole" model, are attractive in that they offer analytic results for the fields and for the power radiated from the antenna. To include the effects of a lossy medium the permittivity is written as

$$\epsilon^* = \epsilon_0(\epsilon' - j\epsilon'') \tag{3}$$

where ϵ_0 is the permittivity of free space, and β is replaced by the propagation constant γ for waves in the lossy medium. γ is given by

$$\gamma^2 = \left(\frac{\omega}{c}\right)^2 \epsilon' \left(-1 + j\left(\frac{\sigma}{\omega\epsilon_0\epsilon'} + \frac{\epsilon''}{\epsilon'}\right)\right) \tag{4}$$

where σ is the conductivity of the medium.

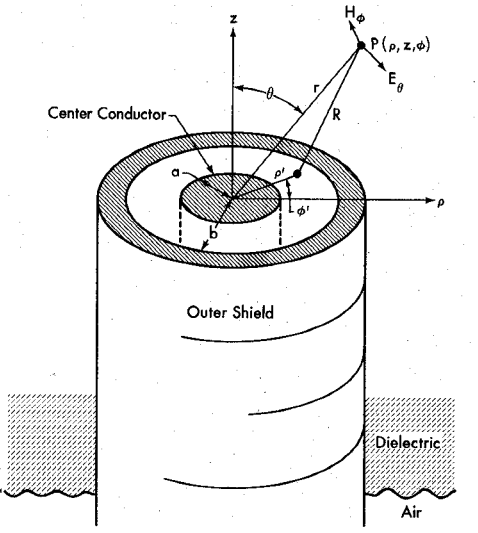

Fig. 1. Geometry of open-ended coaxial antenna.

The current density for the elemental monopole extending along the z axis for a distance Δl can be written as

$$\boldsymbol{J}_s = \frac{I}{\pi\rho_0^2}\hat{\mu}_z \tag{5}$$

where I is the current in the monopole, ρ_0 is the radius of the monopole element, and $\hat{\mu}$ represents a unit vector in the subscripted direction. The electric field produced by such a current element is given by

$$\boldsymbol{E} = j\omega\left(\frac{\nabla(\nabla\cdot\boldsymbol{A})}{\gamma^2} - \boldsymbol{A}\right) \tag{6}$$

$\boldsymbol{A}$, the magnetic vector potential, is related to the current density by

$$\boldsymbol{A} = \frac{\mu}{4\pi}\int \frac{\boldsymbol{J}_s' e^{-\gamma R}}{R} dv' \tag{7}$$

where μ is the magnetic permeability of the medium and R is the distance of the observation point from a point within the monopole volume.

If the dimensions of the dipole element (ρ_0 and Δl) are considered small compared to the distance of the field observation point, (7) and (5) yield the standard result

$$A_z = \frac{\mu}{4\pi} I\Delta l \frac{e^{-\gamma r}}{r}. \tag{8}$$

The electric field in the lossy medium can now be determined by using (6) as

$$E_z = j\omega\mu \frac{I\Delta l}{4\pi}\frac{e^{-\gamma r}}{\gamma^2 r}\left(-\gamma^2 - \frac{\gamma}{r} + \frac{\gamma^2 z^2 - 1}{r^2} + \frac{3z^2\gamma}{r^3} + \frac{3z^2}{r^4}\right) \tag{9}$$

and

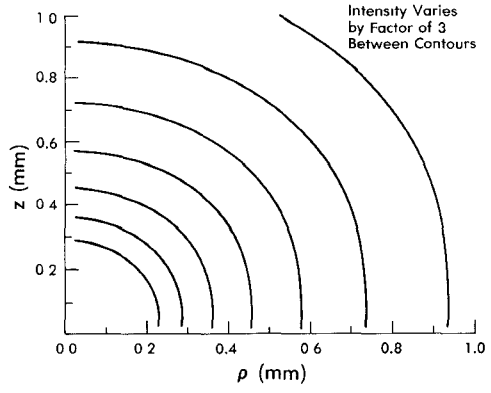

Fig. 2. Power contour plots in the near-field region of a short monopole in a lossy medium. Frequency=2.45 GHz, $\epsilon'=30$, $\tan\delta=0.3$

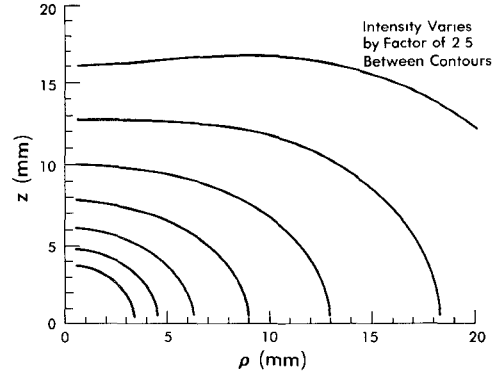

Fig. 3. Power contour plots of a short monopole immersed in a lossy medium showing the emergence of the far-field profile as the distance from the antenna increases. Frequency=2.45 GHz, $\epsilon'=30$, $\tan\delta=0.3$.

$$E_\rho = j\omega\mu \frac{I\Delta l}{4\pi} \frac{e^{-\gamma r}}{\gamma^2 r} \left(\frac{z\rho}{r^2}\right)\left(\gamma^2 + \frac{3\gamma}{r} + \frac{3}{r^2}\right). \quad (10)$$

A_z is independent of ϕ and thus there is no ϕ component of $\boldsymbol{E}$.

Our primary interest is in the energy absorbed in the surrounding medium and thus in $(\sigma+\omega\epsilon_0\epsilon'')|E|^2$. Separating real and imaginary parts of (9) and (10) yields

$$|E|^2 = \frac{(\mu\omega)^2 e^{-2\alpha r}}{|\gamma^2|^2}\left(\frac{I\Delta l}{4\pi}\right)^2 \frac{1}{r^2}\left(\left(1-\left(\frac{z}{r}\right)^2\right)\right.$$
$$\cdot\left(|\gamma^2|^2 + \frac{2\,\mathrm{Re}(\gamma\gamma^{2*})}{r} + \frac{2\,\mathrm{Re}(\gamma^2)}{r^2}\right.$$
$$\left.\left. + \left(1+3\left(\frac{z}{r}\right)^2\right)\left(\frac{|\gamma^2|^2}{r^2} + \frac{2\alpha}{r^3} + \frac{I}{r^4}\right)\right)\right) \quad (11)$$

where

$$\mathrm{Re}(\gamma\gamma^{2*}) = \omega^2\mu\epsilon_0\epsilon'(\beta\tan\delta - \alpha) \quad (12)$$

$$|\gamma^2|^2 = (\omega^2\mu\epsilon_0\epsilon')^2(1+\tan^2\delta) \quad (13)$$

$$\tan\delta = \sigma/(\omega\epsilon_0\epsilon') + \epsilon''/\epsilon' \quad (14)$$

where α and β in (12) are the real and imaginary parts of the propagation constant γ. Contour plots of $(\sigma+\omega\epsilon_0\epsilon'')|E|^2$ in a ρ, z plane are shown in Figs. 2 and 3. Fig. 2 shows a symmetrical absorption of power close to the monopole. In Fig. 3, the expected far-field radiation pattern for a monopole is beginning to emerge.

Unfortunately, although this simple model with its analytic predictions for the fields is attractive, it is unrealistic for predicting the heating patterns to be expected from practical, implantable antennas. Although the power crossing a surface of radius R surrounding the monopole can and has been calculated [11], the results approach infinity as one approaches the origin, and thus any calculation of the total power absorbed within any sphere containing the probe will yield an infinite and incorrect value. This result is not due to the neglect of insulation considerations, as has been suggested [11], but is simply due to the invalidation of the approximation of a small source used in deriving the vector potential in (8).

An alternative approach to understanding the radiation patterns of small coaxial probes is to assume that the center conductor protrudes sufficiently for it to be treated as a quarterwave monopole [6]. This would require the center conductor to protrude by about 20 mm in typical tissue of dielectric constant 40. Such a probe would give an impractically long cylindrical heating pattern for many applications.

II. Equivalent Magnetic Source Method

The approach we finally adopted is an extension of the far-field free-space calculation, described, for example, by Jordan and Balmain [9], in which the surface separating the inner and outer conductor of the coaxial cable is replaced by an equivalent magnetic current sheet. This model does not give analytic results for the fields in the near field even in a lossless medium. We have determined the near field in various lossy media by numerical methods. The fields calculated from this open coax method remain finite in value as one approaches the origin permitting the calculation of the relative total power absorbed in a hemisphere of radius R. The total power radiated from the open-ended coax is assumed constant as the coaxial dimensions and the electrical properties of the medium are varied. The results obtained from this model are really more appropriate for a coaxial line opening into an infinite ground plane; however, calculations reported by Bahl and Stuchly [12] indicate that for an open-ended coaxial probe immersed in a lossy medium, the effect of a finite size ground plane on the input impedance of the probe, at least, are negligible except for very small probes. This is borne out also by dielectric measurements made by inserting open-ended coaxial probes with and without extended ground planes into lossy media [13], [14]. As pointed out by Taylor [4], when implantable coaxial probes lack a ground plane there is an attenuated wave traveling back up the outer conductor but thermographic studies indicate that the effect of this wave in heating is small. Indeed, the experimentally observed heating patterns from such probes are qualitatively exactly what would be expected for radiation into the half space in front of the antenna and thermal conduction both through the surrounding tissue and back along the outer conductor.

In using the equivalent magnetic source method we assume that 1) no current flows on the outside of the cable, and 2) the transverse dimensions of the cable are small compared to a wavelength so that only the TEM mode exists in the coax.

These assumptions imply that both electric and magnetic fields are zero on the outside surface of the cable and thus the only surface contributing to the equivalent current sheet is the annular surface between inner and outer conductor. Over this surface the electric field is radial and strong and the magnetic field is circumferential and to a first approximation zero because of the open-circuit assumption. Therefore, the radiation from the open-ended cable can be calculated using an equivalent magnetic current sheet only. These assumptions are discussed further by Jordan and Balmain (9). Within the framework of these assumptions we believe that this model represents the most realistic approach to the problem of determining energy deposition in lossy media from small coaxial probes. The predictions of the model, as we shall see, are certainly consistent with the small amount of experimental data which is available on the fields and heating patterns of such probes.

The tangential component of the electric field will be discontinuous across the magnetic current sheet. For a magnetic current density $\boldsymbol{M}$, this condition results in the following equation:

$$\boldsymbol{M} = -\boldsymbol{n} \times \boldsymbol{E} \tag{15}$$

where $\boldsymbol{n}$ is the unit normal vector. For the coaxial cable, (15) becomes

$$\boldsymbol{M} = -\hat{\mu}_\phi \frac{V/\ln(b/a)}{\rho} = -\hat{\mu}_\phi \frac{K_0}{\rho} \tag{16}$$

where b and a are the outer and inner dimensions of the coax, respectively, as shown in Fig. 1, and V is the potential difference between the inner and outer conductor. The electric field is related to the magnetic current density through the use of the electric vector potential $\boldsymbol{F}$ by the following equations:

$$\epsilon^* \boldsymbol{E}^m = -\nabla \times \boldsymbol{F} \tag{17}$$

where $\boldsymbol{E}^m$ specifies an electric field derivable from a vector electric potential $\boldsymbol{F}$, and

$$\boldsymbol{F} = \frac{1}{4\pi} \int \frac{\epsilon^* \boldsymbol{M}' e^{-\gamma R}}{R} dv'. \tag{18}$$

Due to the symmetry of the problem the observation point (ρ, z, ϕ) can arbitrarily be taken in the $y-z$ plane so that all y components of the magnetic current will cancel and only the x components will contribute to the field. Inserting (16) into (18) we have

$$F_\phi = -\frac{K_0 \epsilon^*}{4\pi} \int_0^{2\pi} \int_a^b \frac{e^{-\gamma R}}{R} \cos\phi' \, d\phi' \, d\rho'. \tag{19}$$

The electric field can now be derived from the electric vector potential by use of (17) and

$$\nabla \times \hat{\mu}_\phi F_\phi = -\frac{\partial F\phi}{\partial z} \hat{\mu}_\rho + \left(\frac{F\phi}{\rho} + \frac{\partial F\phi}{\partial \rho} \right) \hat{\mu}_z. \tag{20}$$

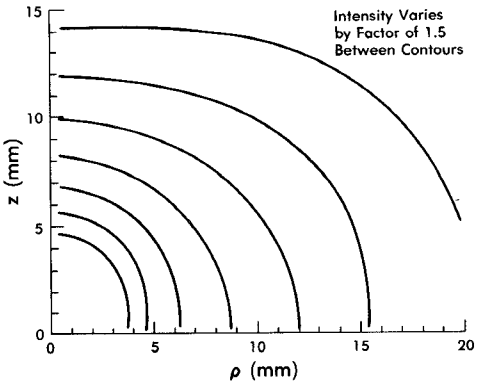

Fig. 4. Power contour plots in vicinity of open-ended coax calculated by equivalent magnetic source method. Frequency=2.45 GHz, $\varepsilon'=30$, $\tan\delta=0.3$, $a=0.4$ mm, $b=2$ mm.

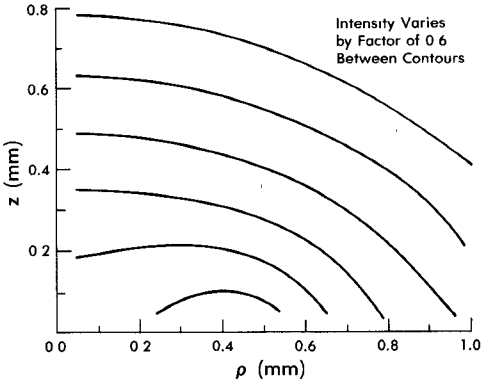

Fig. 5. Power contour plots in vicinity of open-ended coax calculated by equivalent magnetic source method. Frequency=2.45 GHz, $\epsilon'=30$, $\tan\delta=0.3$, $a=0.4$ mm, $b=2$ mm.

If the coordinates of a point on the magnetic current sheet are $(\rho', 0, \phi')$ then the distance R from this point to the point of observation P is found from

$$R^2 = \rho^2 + \rho'^2 + z^2 - 2\rho\rho' \cos\phi'. \tag{21}$$

The two components of $\boldsymbol{E}$ can be expressed as follows:

$$E_\rho = \frac{K_0}{4\pi} \int_0^{2\pi} d\phi' \int_a^b d\rho' \frac{z \cos\phi' e^{-\gamma R}}{R^2} \left(\gamma + \frac{1}{R} \right) \tag{22}$$

$$E_z = \frac{K_0}{4\pi} \int_0^{2\pi} d\phi' \int_a^b d\rho' \frac{\cos\phi' e^{-\gamma R}}{R} \left(\frac{1}{\rho} + \frac{1}{R} \left(\gamma + \frac{1}{R} \right) (\rho' \cos\phi' - \rho) \right). \tag{23}$$

Equations (22) and (23) can be solved fairly easily in the far field by making the simplifying assumption that the R in the denominator can be replaced by

$$R = (\rho^2 + z^2)^{1/2} \tag{24}$$

and in the phase factor by

$$R \cong (\rho^2 + z^2)^{1/2} - 2\rho \sin\theta \cos\phi'. \tag{25}$$

This approach will not work in the near field where (22) and (23) must be integrated directly without further simplification. We have carried out these calculations for a wide range of coaxial line dimensions and media dielectric

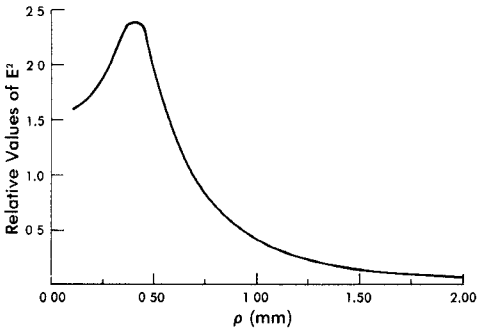

Fig. 6. Variation of the electric field squared calculated by the equivalent magnetic source method. Frequency=2.45 GHz, $\epsilon'=30$, $\tan\delta=0.3, a=0.4$ mm, $b=2$ mm, $z=0.1$ mm.

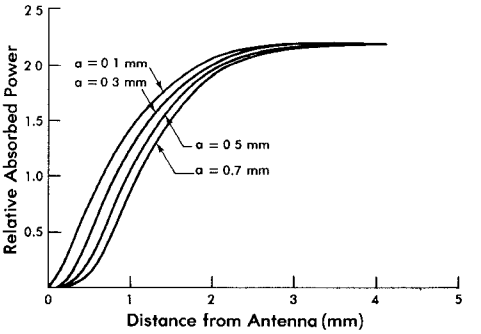

Fig. 8. Relative power absorbed within radius R for various values of the inner radius. Frequency=2.45 GHz, $\epsilon'=30$, $\tan\delta=0.3$, $b=2$ mm.

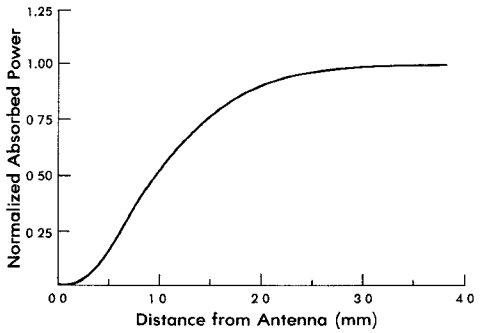

Fig. 7. Normalized power absorbed within radius R. Frequency=2.45 GHz, $\epsilon'=30$, $\tan\delta=0.3, a=0.4$ mm, $b=2$ mm.

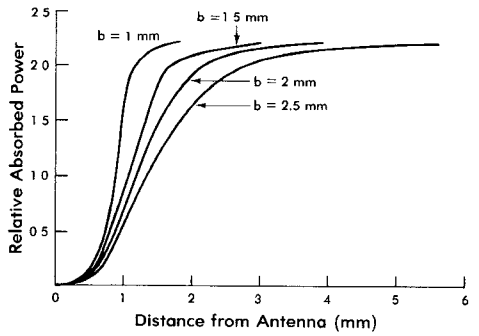

Fig. 9. Relative power absorbed within radius R for various values of the outer radius. Frequency=2.45 GHz, $\epsilon'=30$, $\tan\delta=0.3, a=0.8$ mm.

properties. These calculations, performed to 1-percent accuracy, are very lengthy even on a large computer. Some contours of local absorbed power $(\sigma+\omega\epsilon_0\epsilon'')|E|^2$ resulting from such calculations are plotted in a $\rho-z$ plane and presented in Figs. 4 and 5. Fig. 4 shows contours at distances that are large compared to the dimensions of the coax. These contours are similar to those obtained by the infinitesimal monopole method, in the far field they became exactly the same. However, whereas the fields obtained from the infinitesimal monopole blow up as the antenna is approached, the fields from the magnetic current sheet do not. These fields remain finite and demonstrate the shadowing effect of the center conductor very close to the antenna. This result is further demonstrated in Fig. 6 where a plot of $|E|^2$ versus ρ is given for a constant value of z of 0.1 mm. The point of inflection occurs at a ρ value of 0.4 mm, which is the radius of the center conductor. Because $|E|^2$ for this model remains finite at the origin, calculations of the total power absorbed within a hemisphere of radius R can now be made by further numerical integration. A typical result is given in Fig. 7. For a material with a dielectric constant of 30, a loss tangent of 0.3, and an operating frequency of 2.45 GHz, it is noted that 90 percent of the power is absorbed within a radius of 2 mm. A slight variation in the distribution of absorbed power can be achieved by changing the radius of the inner conductor a. This is shown in Fig. 8.

The variation in absorption with changes in the radius of the outer conductor is shown in Fig. 9. The response to this variation is more dramatic and simply indicates distribu-

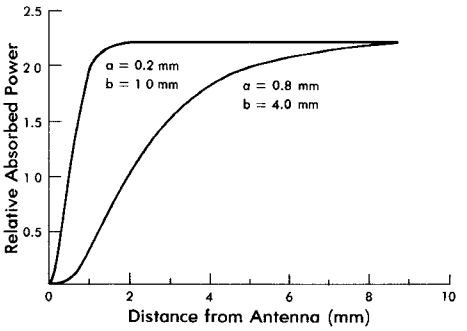

Fig. 10. Relative power absorbed within a sphere of radius R in the vicinity of the small probe. Frequency=2.45 GHz, $\epsilon'=30$, $\tan\delta=0.3$.

tions of the power over a larger volume as the source size is increased. Variation of a single parameter a or b, will cause changes in the characteristic impedance of the line and may cause difficulties in impedance matching. However, both a and b can be varied by the same factor, maintaining the desired characteristic impedance, but causing the larger variation in energy absorption shown in Fig. 9. Power coupling to the medium can be optimized with appropriate tuning stubs. The effect of maintaining line impedance constant but increasing line size is demonstrated in Fig. 10. Increasing the line diameter by a factor of 4 produces roughly a factor of 5 increase in the radius of the hemispherical region within which 90 percent of the power is absorbed.

Variation in the loss tangent does cause considerable variation in absorption, as should be expected. Typical results are presented in Fig. 11. These variations due to

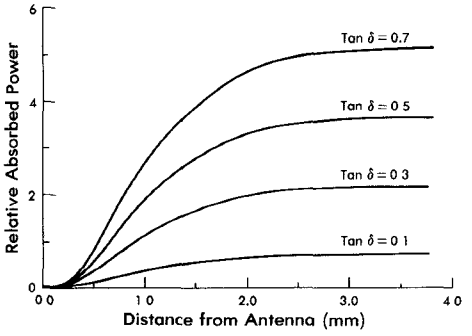

Fig. 11. Relative power absorbed within radius R for various values of $\tan\delta$. Frequency=2.45 GHz, $\epsilon'=30$, $a=0.4$ mm, $b=2$ mm.

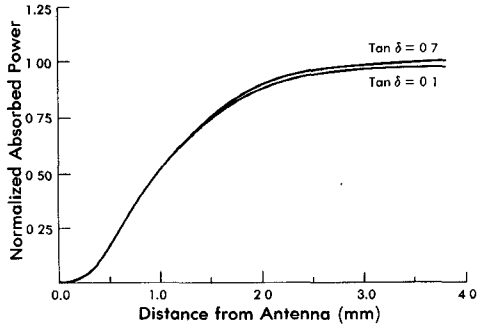

Fig. 12. Integrated values of E^2 within radius R. Frequency=2.45 GHz, $\epsilon'=30$, $a=0.4$ mm, $b=2$ mm.

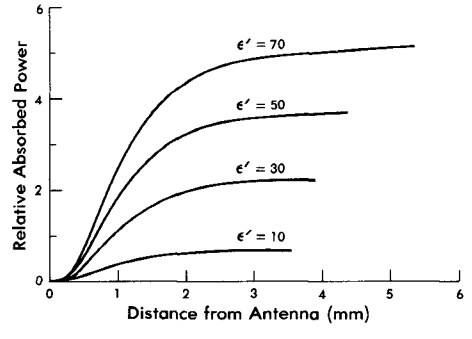

Fig. 13. Relative power absorbed within radius R for various values of ϵ'. Frequency=2.45 GHz, $\tan\delta=0.3$, $a=0.4$ mm, $b=2$ mm.

$\tan\delta$ are almost entirely due to the multiplicative constant ($\omega\epsilon_0\epsilon'\tan\delta$) and not due to variations in $|E|^2$. This is demonstrated by the results presented in Fig. 12 in which the same values used in Fig. 11 are used to calculate numerical values of $|E|^2$.

The response of the relative absorption to the dielectric constant is similar to that of the loss tangent and is presented in Fig. 13.

The variation in $|E|^2$ (not power absorbed) along ρ for a fixed value of z for various parameters of frequency, dielectric constant, loss tangent, a and b are given in Figs. 14–17. As expected from previously presented data, the major variations occur extremely close to the probe center. The variation of $|E|^2$ with ρ for various values of z is given in Fig. 18. These results again indicate large variations close to the origin with more uniform absorption as one ap-

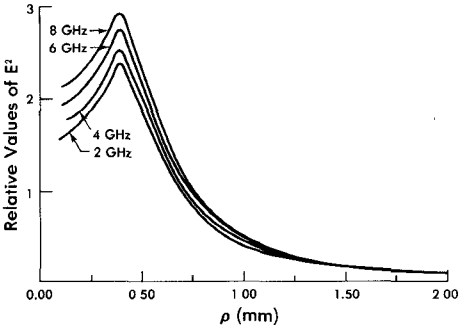

Fig. 14. Variation of the electric field squared for several frequencies as a function of ρ. $\epsilon'=30$, $\tan\delta=0.3$, $a=0.4$ mm, $b=2$ mm, $z=0.1$ mm. Total radiated power is assumed constant and does not depend on antenna impedance match.

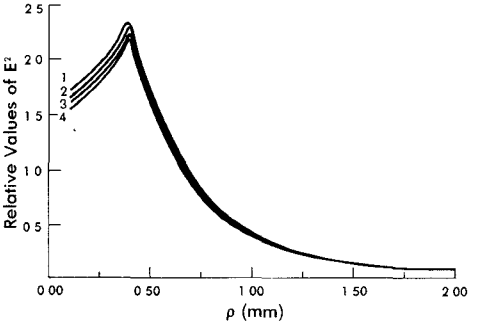

Fig. 15. Variation of the electric field squared for several values of ϵ' as a function of ρ. Frequency=2.45 GHz, $\tan\delta=0.3$, $a=0.4$ mm, $b=2$ mm, $z=0.1$ mm. Values of ϵ', (1)=70, (2)=50, (3)=30, (4)=10. Total radiated power is assumed constant and does not depend on antenna impedance match.

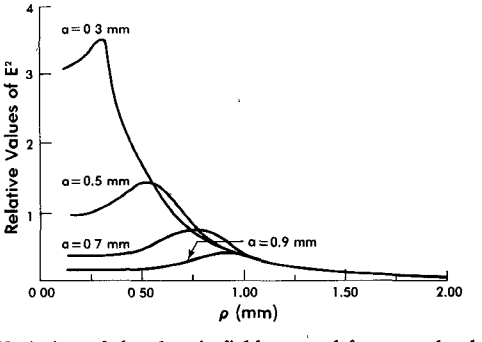

Fig. 16. Variation of the electric field squared for several values of the inner radius as a function of ρ. Frequency=2.45 GHz, $\epsilon'=30$, $\tan\delta=0.3$, $b=2$ mm, $z=0.1$ mm. Total radiated power is assumed constant and does not depend on antenna impedance match.

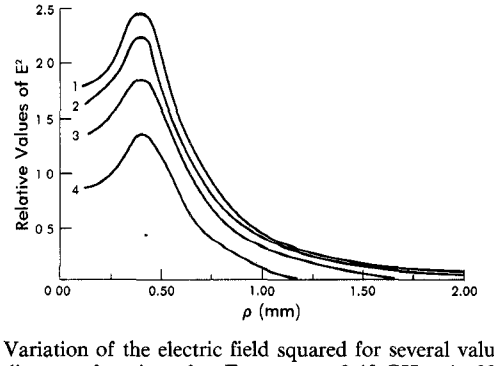

Fig. 17. Variation of the electric field squared for several values of the outer radius as a function of ρ. Frequency=2.45 GHz, $\epsilon'=30$, $\tan\delta=0.3$, $a=0.4$ mm, $z=0.1$ mm. Values of b, (1)=2.5 mm, (2)=2 mm, (3)=1.5 mm, (4)=1 mm. Total radiated power is assumed constant and does not depend on antenna impedance match.

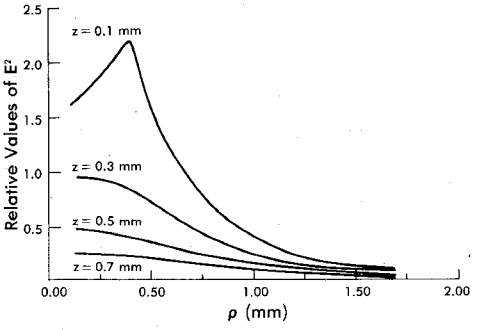

Fig. 18. Variation of the electric field squared for several values of z as a function of ρ. Frequency=2.45 GHz, $\epsilon'=30$, $\tan\delta=0.3$, $a=0.4$ mm, $b=2$ mm. Total radiated power is assumed constant and does not depend on antenna impedance match.

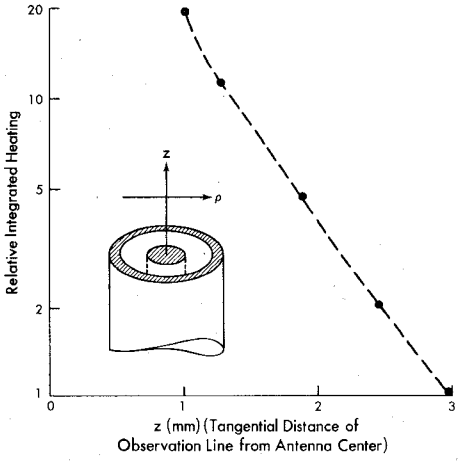

Fig. 19. Variation of the integrated heating produced by an open-ended coaxial probe having $a=0.46$ mm, $b=1.48$ mm. The integrated heating refers to the average energy deposition integrated along a line crossing the antenna axis a perpendicular distance z from the antenna.

proaches dimensions on the order of the outer radius of the coax.

Unfortunately measurements of the near fields of small coaxial probes in lossy media are not available. The closest indirect information about these fields can be deduced from observations reported by us elsewhere [1], where we observed the heating produced in the vicinity of an open-ended coaxial antenna in lossy liquids by an optical heterodyne method. In these experiments pulsed microwave irradiation was used so the results were negligibly affected by thermal conductions. Our observations indicated negligible heating near the outer conductor below the plane of the open end (in the geometry of Fig. 1) and showed a drop off in heating in the z direction which was entirely consistent with the theory presented here. The extent of heating can be deduced from results such as Fig. 19 which essentially shows values of $(\sigma+\omega\epsilon_0\epsilon'')|E|^2$ integrated in the ρ direction past the antenna at various values of z.

III. Conclusions

We have presented details of calculations of the near fields of an open-ended coaxial antenna in various lossy media. The model used, where the annular region between inner and outer conductor at the end of the coax is replaced by an equivalent magnetic current sheet, yields results which remain finite as the antenna is approached. This allows calculation of the total power absorbed within a hemispherical region around the end of the antenna to be made which cannot be made for infinitesimal or short monopole models whose fields blow up at the antenna. We have presented results which show the extent of medium heating for several antenna sizes and media dielectric properties. These results should be of use to workers interested in implantable antennas for cancer therapy by microwave hyperthermia. We have presented our calculations for a frequency of 2.45 GHz, the most commonly used value for hyperthermia; our results can be easily extended to other frequencies by scaling. The principal simple result of our calculations is that in lossy media the bulk of the power is absorbed within a radius of the antenna of the order of the radius of its outer conductor.

Our model does depend on certain assumptions [9]; principally that the fields are essentially the same in the presence of a small finite ground plane as they would be in the case of an extended ground plane. In this context experimental measurements [14] indicate that the difference between the impedances of such an antenna embedded in a lossy media with and without a ground plane are negligible.

References

[1] C. C. Davis and M. L. Swicord, "Studies of microwave absorption in liquids by optical heterodyne detection of thermally induced refractive index fluctuations," presented at URSI Conference Helsinki, Finland, Aug. 1978; to be published in *Radio Science*.

[2] C. C. Davis, and M. L. Swicord, "Studies of microwave absorption in liquids by phase fluctuation optical heterodyne spectroscopy," in *Proc. Bioelectromagnetics Symp.*, Seattle, WA, June 1979.

[3] L. S. Taylor, "Electromagnetic syringe," *IEEE Trans. Biomed. Eng.*, vol. BME-25, pp. 308–309, May 1978.

[4] ——, "Implantable radiators for cancer therapy by microwave hyperthermia," *Proc. IEEE*, vol. 68, pp. 142–149, Jan. 1980.

[5] E. B. Douple, J. W. Strohbehn, E. D. Bowers, and J. E. Walsh, "Cancer therapy with localized hyperthermia using an invasive microwave system," *J. Microwave Power*, vol. 14, pp. 181–186.

[6] J. W. Strohbehn, E. D. Bowers, J. E. Walsh and E. B. Douple, "An invasive microwave antenna for locally-induced hyperthermia for cancer therapy," *J. Microwave Power*, vol. 14, pp. 339–350.

[7] H. Bassen, P. Herchenroeder, A. Cheung, and S. Neuder, "Evaluation of an implantable electric-field probe within finite simulated tissues," *Radio Science*, vol. 12, pp. 15–25, 1977.

[8] E. C. Burdette, F. L. Cain and J. Seals, "In vivo probe measurement technique for determining dielectric properties at VHF through microwave frequencies," *IEEE Trans. Microwave Theory Tech.*, vol. MTT-28, pp. 414–427, 1980.

[9] E. C. Jordan and K. G. Balmain, *Electromagnetic Waves and Radiating Systems*. New York: Prentice–Hall, 1968, pp. 490–493.

[10] R. F. Harrington, *Time Harmonic Electromagnetic Fields*. New York: McGraw–Hill, 1961, pp. 110–113.

[11] J. R. Wait, "Electromagnetic fields of sources in lossy media," in *Antenna theory Part II*, Collin and Zuecher, Eds. New York: McGraw–Hill, 1969.

[12] I. J. Bahl and S. S. Stuchly, "The effect of finite size of the ground plane on the impedance of a monopole immersed in a lossy medium," *Electronics Lett.*, vol. 15, pp. 728–729, 1979.

[13] T. W. Athey, M. A. Stuchly, and S. S. Stuchly, "Dielectric properties of biological substances at radio frequencies. Part I-Measurement method," to be published.

[14] P. D. Hrycak, "Microwave dielectric constant measurement system for in-vivo tissue," Masters thesis, University of Maryland, 1979.

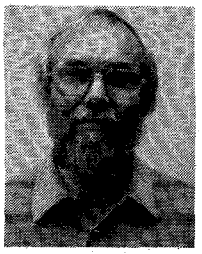

Mays L. Swicord was born in Chunju, Korea, on May 5, 1938. He received the B.A. degree from King College, Bristol, TN, in 1960 and the M.S. degree from the University of North Carolina in 1963. He received the Ph.D. degree from the University of Maryland in 1980. His doctoral research involved studies of microwave absorption by liquids and liquid solutions of biological materials.

From 1963 to 1965, he was an instructor of physics at Davidson College, Davidson, NC, and from 1965 to 1969 he was employed in the private sector where his work included studies of electromagnetic propagation, evaluation of radiation damage to semiconductor devices and design of specialized filters and antennas.

He is now a senior scientist at the Bureau of Radiological Health, Rockville, MD, where has been employed for the past 12 years. His administrative and research activities have included the establishment of a unique microwave power density calibration facility, development of instrumentation for nonperturbing electric field measurements, development of wide band dielectrometry techniques and methods. His recent work involves using optical heterodyne techniques for determining microwave absorption in biomolecules. Dr. Swicord is a member of the Bioelectromagnetics Society.

Christopher C. Davis was born in Manchester, England, on July 7, 1944. He received the B.A. and M.A. degrees from Trinity College, Cambridge, England, in 1965 and 1970, respectively, and the Ph.D. degree in physics from the University of Manchester, England, in 1970. His doctoral research involved studies of excitation and relaxation processes in noble-gas lasers.

From 1969 to 1973, he was a Research Associate in the Department of Physics at the University of Manchester, where he carried out research on atomic-iodine gas-discharge lasers, electronegative plasmas, and atomic-iodine photodissociation lasers. From 1973 to 1975, he was a Research Associate with the Materials Science Center, Cornell University, Ithaca, NY, where he carried out research on molecular energy transfer and relaxation. Since 1975, he has been at the University of Maryland, College Park, where he is now Associate Professor of Electrical Engineering. His current research interests include bioelectromagnetics, particularly with regard to basic physical mechanism for interaction of nonionizing radiation with biological systems, applications of optical heterodyne techniques to the study of physical and chemical phenomena, and molecular energy transfer and relaxation.

Dr. Davis is a member of the Bioelectromagnetics Society and the Institute of Physics (London).

Dielectric Loss in Biogenic Steroids at Microwave Frequencies

R. ARUNA AND J. BEHARI

Abstract—**Dielectric loss in steroids has been measured in solid form at 9.4 GHz and in nonaqueous solutions at 3.3 and 9.4 GHz. The method for solutions consists of measurement on standing-wave pattern in front of a column of liquid of varying length and concentration, contained in a short-circuited dielectric cell. Keeping the concentration within the limits of dilute solutions, dipole moment and relaxation time of Cholesterol, Progesterone, and Testosterone have been evaluated. Mechanisms responsible for dielectric loss and its trend of variation in the three steroids are presented. The solid phase measurements were carried out by cavity perturbation technique on powders and crystal values for ϵ' and ϵ'' were evaluated. The difference in ϵ'' values of the three steroids in the two phases is attributed to the difference in the mechanism of microwave absorption. However, identical values of ϵ' are obtained.**

I. Introduction

THE EFFECT OF microwaves on biological systems has assumed an interesting dimension in recent years [1], [2]. This is largely due to increasing use of microwaves in medical diagnosis and therapy. The energies of microwave quanta rule out the possibility of direct effects, such as intermolecular bond breaking or intramolecular alterations at the molecular level, that are produced by ultraviolet and other ionizing radiations.

The propagation characteristics of electromagnetic waves through a biological medium depends upon its electrical properties. The significant electrical property of a system which determines the impedance offered to the incident wave is the electric permittivity of the medium [3]. Since all biological media are lossy, attenuation occurs as energy is absorbed. Attenuation and accompanied phase shift are dependent on the dielectric properties of the medium characterized by complex permittivity ϵ^* of the medium denoted as $\epsilon'-j\epsilon''$. The possible biological effects of microwave exposure can be evaluated quantitatively by considering the probable molecular interactions with biomolecular liquids. This requires, besides loss tangent, an evaluation of relaxation time and dipole moment. Dipole moment is a direct measure of charge asymmetry, while relaxation time provides information regarding the immediate environment of the molecule. To isolate the effect of the solvent, we have determined the complex permittivity in crystalline form as well.

Most of the work pertaining to biological effects of microwaves are measurements on tissues or on composite

Manuscript received April 6, 1981; revised July 13, 1981. This work was supported in part by ICMR, India.

The authors are with the School of Environmental Sciences, Jawaharlal Nehru university, New Delhi—110067, India.

0018-9480/81/1100-1209$00.75 ©1981 IEEE